A Model Independent Scheme of Adaptive Focusing for Wireless Powering to In-Body Shifting Medical Device

Zaiping Nie, *Fellow, IEEE*, and Yuan Yang

***Abstract*—A novel method for wireless power transfer (WPT) in complex multipath propagation environments of human body, based on the reversal pretest and the principle of reciprocity, has been proposed in this paper to adaptively enhance the intensity of the field on the surface of implanted antenna. As a model-independent scheme, this method makes all the field components focus adaptively on a given position in unknown inhomogeneous media which can be very complicated, random, and even time varying. The principle and the steps of the adaptive focus (AF) WPT are described first. The design of the implanted antenna conformal with a capsule inside the tissue and the multiple antennas out of the body is then given to build a principled prototype for the AF-WPT. Both the numerical simulation and the experimental measurement for the AF-WPT model with the operation frequency in Industrial Scientific Medical Band have been given to show the validation of this method. It has been shown from the simulation and experimental results that in comparison with the other methods, the field focusing scheme increases 6 dB higher intensity of the field at the position of the capsule antenna while keeping the level of the received power more stable with the continuous shifting of the implanted antenna.**

***Index Terms*—In-body medical device, wireless power transfer (WPT), wireless powering to moveable capsule endoscope.**

I. Introduction

IN RECENT years, various types of electronic apparatus have been implanted in human body for medical sensing, medicine delivery, and local stimulation. These devices help manage a broad range of medical disorders through preventive and postsurgery monitoring. In order to avoid the risks associated with the battery exhausting and replacing, and to reduce the size of the medical device, the wireless delivery of energy has been proposed as a key technology for application of those devices [1]. The traditional way for wireless power transfer (WPT), including electromagnetic (EM) coupling [2]–[5] and magnetic resonance coupling [6]–[9], is based on the EM near-field coupling with relatively low operation frequencies (several megahertz, for example) and share of the magnetic flux between the transmitting and receiving terminals. Konno *et al*. [10] improved the coupling coefficient by redesigning and adjusting the inner radius of the spiral coil. Miwa *et al*. [11] improved the transmission efficiency by using the coil array. Awai *et al*. [12] applied the magnetic coupling to reduce the dielectric loss appreciably. Jonah *et al*. [13], [14] designed a 3-D loop structure to address the misalignment between the external source and the pickup coils of the implanted device which causes the considerable degradation of the coupling efficiency. However, the large size of the implanted coil and the rigid requirement of the alignment may still pose severe challenges to the technology of the near-field coupling [15].

Recently, the WPT techniques with operation frequency from sub- to low GHz have been drawing attention due to their much higher transfer efficiency than that of conventional near-field coupling [16]–[18]. This kind of WPT techniques, including EM radiation, multipath propagation, and receiving, may be interpreted as an interference-based WPT. Among the relevant works, a new antenna design, called patterned metal plate, is used to form highly directive propagation modes for millimeter sized coil to receive the energy in a given multilayer geometry [19]. Based on the closed-loop feedback relayed over an optical fiber, a "greedy phase search algorithm" has been implemented to remove the dark regions of the fields resulted from the rhythmic motion of the implanted device due to breathing and heartbeat of bodies [20].

A conjugate matching scheme based on the reciprocity theorem has been proposed to focus EM energy in tumor area for hyperthermia application [21]. However, this scheme failed to focus the field in the entire domain of the tumor but only on the surface of the probe because only the probe surface is the area with the reciprocity of the sources and the fields in this scheme. As the result, the field and EM energy in most volume of the tumor are still very weak. Furthermore, the experiment in this paper does not treat any biological tissue as the focus area but simply experiments with EM wave radiation and receiving in a water tank. Therefore, this experiment has not proved the proposed concept. Finally, the whole media environment has been changed and the reciprocity relationship is no longer valid when the probe and its feeding line are removed from the tumor for preparing the hyperthermia step. It is also noted that this scheme has to introduce a probe with

Manuscript received May 11, 2017; revised December 14, 2017; accepted December 30, 2017. Date of publication January 17, 2018; date of current version March 1, 2018. This work was supported in part by the Natural Science Foundation of China under Project 61231001 and 61721001, in part by the China Central Universities Fundamental Research Special under Project ZYGX2010J024, and in part by the Youth Fund of Natural Science Foundation of China under Project 61201281. *(Corresponding author: Zaiping Nie.)*

The authors are with the School of Electronic Engineering, University of Electronic Science and Technology of China, Chengdu 611731, China (e-mail: zpnie@uestc.edu.cn; yanyner@foxmail.com).

Color versions of one or more of the figures in this paper are available online at http://ieeexplore.ieee.org.

Digital Object Identifier 10.1109/TAP.2018.2794385

feeding line into tumor, which causes additional injury to the pathological tissue.

In summary, most of the efforts made before fall into the category of partial improvements, for example, the optimum design of the antennas, introduction of the layered media to model the influence of body tissue, and so on. However, the optimum designs of the antennas lose their route and guidance without the real multipath figure of the field penetrating into the human body. Furthermore, as the model-dependent schemes, they are not very meaningful because different models will lead to different results and different conclusions. Obviously, the simplified models are not appropriate for simulating real human body, and any realistic human body is difficult to be modeled exactly due to its inherent complexity. Moreover, the modeling of human body has to face different sizes and different figures of different people. In other words, we cannot find a model generally suitable for every people, which is an inevitable challenge for the model-dependent methods.

Actually, the wireless propagation in inhomogeneous human body always results in the multipath fading, which corrupts the transmission efficiency severely but is always ignored in most research reports. Furthermore, to ensure that the rechargeable batteries receive EM energy effectively, all the wave components which have arrived at the position of the medical device should be superimposed in-phase. Therefore, it makes the focused field strong enough in the position of the implanted antenna. The field focusing is particularly important for implanted antenna at small size. If the multipath field components are not focused on the antenna, they are probably propagate to elsewhere, and a lot of EM energy is wasted consequently, which results in EM pollution to the human tissue. Unfortunately, there is little work about the technique of the field focusing in inhomogeneous body media in the previous literature.

The technique of the field focusing for WPT to human body is facing a lot of challenges. First, as the wireless propagation media, the human bodies are difficult to be modeled properly due to their individual differences, i.e., the models strongly depend on the different sizes and figures of the human bodies. Furthermore, the implanted medical device may keep shifting inside the body and is very difficult to be located in real time. In other words, the field focusing should be conducted without the information about the inhomogeneity of the propagation environment and the position of the medical device to be charged.

In this paper, a novel approach for WPT in complex multipath environments (in human body, for example), based on the reversal pretest and the principle of reciprocity, has been proposed to adaptively focus and enhance the field in the position where the antenna of the medical device locates. By means of this method, the waves propagate and focus adaptively on the given position in unknown complex inhomogeneous media which can be very complicated, random, and even time varying. The model for WPT, including the multiple antennas out of the body and a conformal capsule-type implanted antenna inside the tissue, all working at the same frequency, has been built and simulated. The numerical results have shown the satisfactory performance of the proposed scheme.

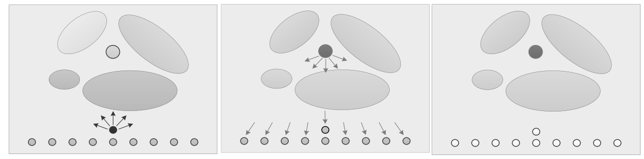

Fig. 1. Basic scheme for the TR mirrors. (a) EM waves launched from the transmitting antenna. (b) Field scattered by target is received by multiple antennas. (c) Simulation of the TR radiation. The field components focus at the target place.

The rest parts of this paper have been arranged as follows. The second part introduces the adaptive focusing approach and its physical principles. The simulation model of the adaptive focus (AF) WPT and the antennas design have all been given in Section III. The numerical examples and the simulation results have been presented in Section IV to show the performance of the AF WPT. The experiment has been given in Section V to validate the proposed scheme. Some discussions and conclusions have been made in the final section.

II. Adaptive Focusing Method for WPT in Inhomogeneous Media

To form the focused field with enough strength in the area where the antenna of the rechargeable battery locates, a feasible way is the near-field focus (NFF) technology. However, various kinds of NFF are not designed for the complex inhomogeneous media such as the human body but mainly for homogeneous background media. The basic task of the field focusing in heterogeneous media is to control the phase of the current feeding to each element of the transmitter multiple antennas, so that the in-phase superposition of all the components in the position of the battery antenna can be realized. However, the EM field is very difficult to be focused in unknown, complex inhomogeneous, and even time-varying environments, because the proper phase data of the current feeding to each antenna element are hard to be determined in advance. Furthermore, there is no "universal" model available for every human body in the context of simulation due to individual difference. To solve these challenges, the AF-WPT (AF-WPT) scheme has been proposed based on the time reversal (TR) concept.

A. Time Reversal (TR) Concept and Its Applications in Electromagnetic Probing and Communications

In 1989, Fink *et al*. [22] proposed the TR imaging concept, called "TR mirrors," for acoustic probing in inhomogeneous media. Since then many reports about the TR method applied to the EM target imaging and the point-to-point wireless communications can be found [23]–[25]. The TR imaging consists of the following three basic steps, as shown in Fig. 1. First, the transmission antenna (in front of the 1-D linear array) radiates an initial wave to "illuminate" the target to be detected in given inhomogeneous media, as shown in Fig. 1(a). Then, the target scatters the incident wave, which results in a backscattered field received by all the antenna elements of the 1-D array of the multiple antennas, as shown in Fig. 1(b). The waveforms of the signals received by each element and their relative time delay have all been measured. Finally, each element of the multiple antennas "retransmits" the signal with the same waveform and the "negative" time delay as that measured previously in the corresponding numerical modeling. As the result, all the wave components which have arrived at the target place will be superimposed synchronously, thus leading to the remarkable enhancement of the field intensity. It should be noticed that the last step is not the real physical process but only the numerical simulation to calculate the field distribution where the points with the field focusing show the locations of the potential targets to be detected.

However, the technical bottleneck of the TR imaging is the difficulty to get Green's function of the inhomogeneous background media for numerical simulation. Actually, the inhomogeneous background media are usually unknown and too complicated to be modeled properly, which leads to the distortion of the calculated field distribution and the target imaging, even to the false alarm or the failure to alarm.

When the TR method is applied to the point-to-point communication, the two-way communications share the same inhomogeneous propagation media without any demand of the modeling. However, the signal transmitted in one (the up-going, for example) channel may not be the same as that in the opposite (down-going) channel in both the waveform and the bandwidth. The remarkable difference between the signals in the up-going and down-going channels may lead to invalidation of the reciprocity. In other words, the in-phase superposition of the multipath components may be failed due to the influence of multipath during the wave propagation and the media dispersion for broadband signals. Consequently, the bit error rate increases, and the quality of service decreases, especially in the case of broadband communications.

Fortunately, in the AF WPT scheme Green's function for the unknown inhomogeneous background media is not required, unlike that in TR imaging**.** Similarly, unlike that in high-speed communication system, the wideband signals with precise coding are not required in the WPT scheme. The wave for wireless powering is generally the narrowband signal. Therefore, the TR concept can be applied successfully to the wireless powering for the medical device in human body with good performance of the field focusing. As an ideal application of the TR concept, the proposed AF-WPT scheme for the moveable device in human body will show its distinguished advantages.

B. Adaptive Focusing Scheme for Wireless Powering to In-Body Medical Device

Assume the sources (J_0, M_0) and (J_k, M_k) locate in source areas P_0 and P_k and excite the field (E_0, H_0) and (E_k, H_k), respectively. According to the reciprocity principle, we have

$$\langle \mathbf{E}_k, \mathbf{J}_0 \rangle - \langle \mathbf{H}_k, \mathbf{M}_0 \rangle = \langle \mathbf{E}_0, \mathbf{J}_k \rangle - \langle \mathbf{H}_0, \mathbf{M}_k \rangle \qquad (1)$$

where the inner product is defined as

$$\langle \mathbf{E}_i, \mathbf{J}_j \rangle = \int_v \mathbf{E}_i \cdot \mathbf{J}_j dr$$

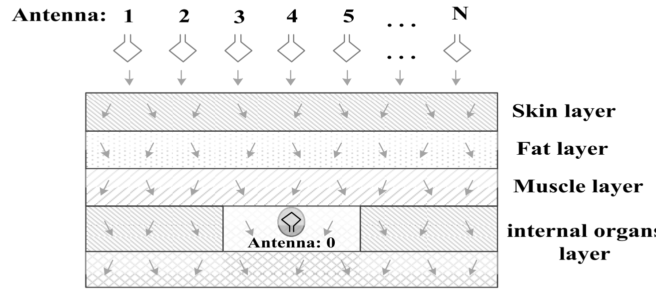

Fig. 2. Multiple path model of the wave propagation for WPT ring to implanted antenna on the medical device.

The volume integrals in above expressions are all defined in the volume where both the source and the field in the integrand are not zero. Therefore, (1) can be expressed in the following form, similar to the formula in [26]:

$$\int_v (\mathbf{E}_k \cdot \mathbf{J}_0 - \mathbf{H}_k \cdot \mathbf{M}_0) dv' = \int_v (\mathbf{E}_0 \cdot \mathbf{J}_k - \mathbf{H}_0 \cdot \mathbf{M}_k) dv' \quad (2)$$

Considering there is no magnetic current in the body media, one can rewrite (1) in a much simpler form as follows:

$$\int_v \mathbf{E}_k \cdot \mathbf{J}_0 dv' = \int_v \mathbf{E}_0 \cdot \mathbf{J}_k dv' \qquad (3)$$

Equation (3) describes the reciprocity between two sources and their fields. In general, only the amplitude relationship in (3) is mostly concerned about, and the phases and the polarizations relations are always ignored. However, the reciprocity of the phases and the polarizations serves as the basis of the AF-WPT.

Let the complexes J_0 and J_k in (3) equal to each other, i.e., $J_0 = J_k = J$ with the same reference phase (of 0°, for example). If the source J at Point P_0 excites the field E_k at Point P_k, then moving J from P_0 to P_k, we can see from (3) that the resulted field E_0 at P_0 is same as E_k in amplitude, and all the fields have phase delay $-\Delta\Phi_k$ compared to that of their sources. If we hope that E_k at P_0 resulted by J_k at P_k still has the phase of 0°, its source J_k at P_k should be previously added with an additional phase leading $+\Delta\Phi_k$. Similarly, as the reversal pretest, the fields E_k at the points P_k ($k = 1, 2, 3, \ldots, K$), all excited by the source J_0 at point P_0, have their phase delays $-\Delta\Phi_k$ compared to that of J_0, respectively. Then, the sources J_k, added previously with the phase leadings $+\Delta\Phi_k$ and moved from P_1 to P_k, will result in E_k with the same phases 0° at Point P_0, respectively. In other words, if the K sources J_k ($k = 1, 2, 3, \ldots, K$) with the phase leading $+\Delta\Phi_k$ at source points P_k of the 1-D linear array, as shown in Fig. 2, radiate synchronously, the total field at P_0 is the in-phase superposition of the K-field components with the identical phases, showing the remarkable gain of the field intensity.

In AF-WPT scheme shown in Fig. 2, Antenna 1, 2, …, N, all locate above the body surface as the multiple antennas, and only Antenna 0, as the implanted antenna, locates inside the human body. And the layered media are used to model the body tissues.

The proposed adaptive focusing scheme consists of the following two basic steps. The first is the pretest step.

TABLE I
THICKNESS AND THE PARAMETERS OF THE HUMAN TISSUES

Tissues	Skin	Fat	Muscle	Bone	Intestine
Thickness (mm)	2.0	10.0	8.0	16.0	40.0
ε_r	30.66	8.32	48.73	8.88	54.43
σ (S/m)	0.70	0.37	2.34	0.45	3.17
tan δ	0.17	0.33	0.35	0.38	0.43

The implanted antenna transmits a pretest signal to the outside multiple antennas once the outside antennas radiate a signal without the field focusing to wake up the implanted device. And then, Antenna 1, 2, …, N receive the pretest signals coming from the implanted antenna, respectively. Assuming that the initial phase of the signal radiated from Antenna 0 is φ_0, and the signals which have arrived at and been received by Antenna 1, 2, …, N have their phase delay of φ_1, φ_2, …, φ_N, so the total phase delays of the signals received by Antenna 1, 2, …, N are $\varphi_0 + \varphi_1$, $\varphi_0 + \varphi_2$, …,$\varphi_{0+}\varphi_N$, respectively.

The second is the WPT step. Let Antenna 1, 2…, N radiate simultaneously the signals with their phase exceeding $-(\varphi_0+\varphi_1)$, $-(\varphi_0+\varphi_2)$, …, $-(\varphi_0+\varphi_N)$, respectively. According to the theorem of reciprocity, the signals which have arrived at the location of Antenna 0 have their phases 0°, the same with each other, thus leading to the in-phase superposition of all the components and the remarkable enhancement of the field amplitude in the focusing area.

Specifically to WPT for biomedical applications, in the first (pretest) step'C Antenna 0 on the medical device embedded in deep tissue sends a test signal first, and then the multiple antennas outside the human body, i.e., Antenna 1, 2, …, N, receive this signal and measure its phase delay. In the second (WPT) step, the multiple antennas outside the human body retransmit the wave with the phase conjugated to that measured in the pretest step (i.e., the absolute value invariant but with the opposite sign). According to the reciprocity theorem, all the components of the field, which are retransmitted by the multiple antennas, are superimposed with the same phase at the position of antenna 0 [27]. Consequently, a focusing area is formed, and the intensity of the field is therefore much higher than that formed by in-phase feeding.

III. SIMULATION MODEL OF ADAPTIVE FOCUS WPT

In this section, a basic simulation model for WPT, where a capsule endoscope is moving in the digestive tract of human body, has been built to evaluate the performance of the proposed WPT scheme.

A. Model of Abdominal Wall of Human Body

In this model, the abdominal wall of the human body is simulated with the multilayered tissues same as that in [17] for the purpose of the performance comparison. The thickness and the electrical parameters of the different layers are all shown in Table I. The parameter values of the corresponding tissues at 2.45 GHz are quoted from [28]–[29].

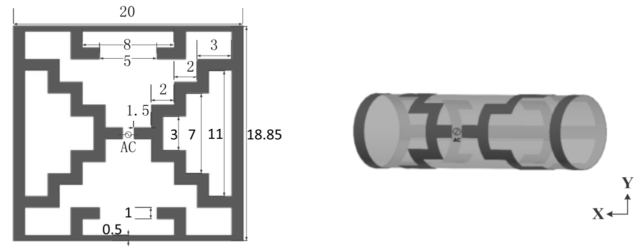

(a) (b)

Fig. 3. Geometry and dimensions of the implanted antenna made on surface of capsule endoscope. (a) Stretch out view and dimensions of the proposed antenna (in mm). (b) 3-D model of implanted antenna conformal with cylinder shaped glass capsule.

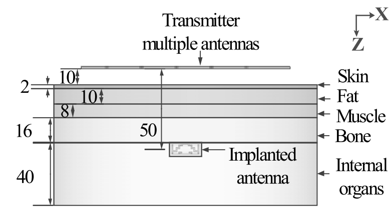

Fig. 4. Layered media model for human body simulation (unit in mm), where x and z stand for directions of body length and thickness, respectively.

This model can be interpreted as a simplified model of the abdominal wall of realistic human body due to its same parameters as the realistic tissues of the abdominal wall. Although only a simplified model of the abdominal wall has been used in the numerical simulation, conclusions are still valid because the AF-WPT scheme is a model independent. Therefore, a real and accurate model of human body is no longer essential for validating the scheme.

B. Implanted Antenna

A folded dipole antenna has been designed as the antenna of a capsule endoscope for WPT application. The antenna is made of conducted strips wrapped on the glass capsule with 6 mm diameter, 20 mm length, and 5 of ε_r. Fig. 3 shows the geometry and dimensions of the proposed antenna, including the stretch out view in Fig. 3(a) and the 3-D model in Fig. 3(b). The antenna is designed to enlarge its electrical size in limited space, while still maintains the full polarization characteristic as much as possible. Fig. 4 shows the parameters of the planarly layered media for modeling the abdominal wall of human body and the position of the implanted antenna. The reflection coefficient (S_{11}) of the implanted antenna has been calculated and its value varying with the frequency is shown in Fig. 5. It can be seen from Fig. 5 that the reflection coefficient at 2.45 GHz (the operation frequency) is about −17 dB, showing a good impedance matching to the feeding line.

C. Multiple Antennas Outside Human Body

To design the multiple antennas outside the human body, the type and number of the antenna elements, the size of the radiation aperture, and the interval between the aperture,

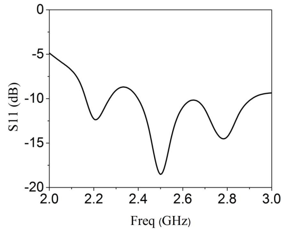

Fig. 5. Reflection coefficient of the proposed implanted antenna in multilayer model of tissue.

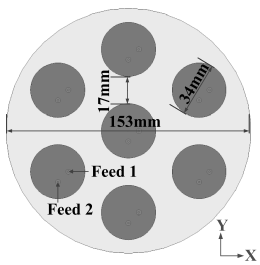

Fig. 6. Geometry of the multiple antennas with seven elements outside human body (unit: mm).

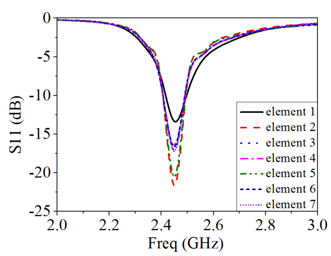

Fig. 7. Reflection coefficient of each element of the multiple antennas.

and the surface of human body, etc., should be determined. Considering that the focus of this section is not the optimum design but the validation of the AF-WPT scheme, we propose only a basic model for simulation. The proposed multiple antennas outside body consist of seven elements of the circular patch microstrip antenna distributing uniformly on an FR-4 circular substrate with 153 mm of diameter and 1.6 mm of thickness. Each antenna element has been designed with two feeding ports to get the characteristics of the dual perpendicular polarizations. The substrate with its electrical parameters $\varepsilon_r = 4.4$ and $\tan\delta = 0.02$ is chosen for design of the multiple antennas. The dimensions of this multiple antennas are all shown in Fig. 6, and the reflection coefficient of each antenna element is shown in Fig. 7. Generally, the multiple antennas are set right above the abdominal cavity when the patient extends his body on the bed, as shown in Fig. 4. Different from the traditional phase collocation of the antenna array, the phase of the signals feeding to each antenna element should be tunable independently, and adjusted to meet the conjugate of the phase delay in the pretest step. As the result of the wave interference, all the wave components arriving at the position of the implanted antenna will be focused and enhanced remarkably, leading to a much more efficient power delivery.

TABLE II
Phases of Current Feeding to Each Element of Multiple Antennas in Case of Capsule Antenna at Its Start Point of Track

Element / Port	1	2	3	4	5	6	7
Port 1_{st}	-9.2	66.0	153.2	152.5	64.2	150.5	155.4
Port 2_{ed}	-102.5	-81.8	-34.98	42.7	-7.7	-135.1	46.2

IV. Simulation Results

The numerical simulation of the WPT based on the model mentioned above has been conducted to obtain the field distribution in the tissue and validate the adaptive field focusing method. The operation frequency in the modeling is actually not critical but we choose it as 2.45 GHz within Industrial Scientific Medical Band for the purpose of comparing the performance of our WPT scheme with that of the previous works. Considering the model for human body is inhomogeneous, the finite-element method has been applied as the simulation tool [30], [31].

A. Evaluation of WPT Efficiency

The WPT efficiency is defined as the ratio of the EM power received by the implanted antenna and the total power radiated from the multiple antennas outside the human body in the power transmission process. The power received by the implanted antenna can be calculated with the voltage at its output terminal and the impedance of the matching load. However, the WPT efficiency has to be evaluated under the condition of the adaptive field focusing.

In the numerical model, the transmission multiple antennas are assumed to be located on the top of the abdominal, and the first position of the implanted antenna is right underneath the central point of the multiantenna aperture, as shown in Fig. 4. In the pretest step, the phase data of the signal received by each antenna of the multiple antenna system should be measured in practical operation. However, the phase data have been calculated in numerical simulation instead of being measured as is shown in Table II. In the WPT step, each antenna element has been fed by the current with the phase conjugated to the phase delay measured in the pretest step. The field distribution on the profile of the human body has been calculated and shown in Fig. 8. It can be seen from Fig. 8 that the electric field on the surface of the implanted antenna of AF-WPT is much more intensive than that of the equiphase feeding, since different components of the electric field have been superimposed in-phase on the surface of the implanted antenna. Actually, the proposed method makes WPT more concentrated so that the field amplitude in position of the implanted antenna is 6 dB higher than that by equiphase feeding, as shown in Fig. 9(a).

In this example, 500 mW of the radio power is assumed to be fed to the multiple antennas, which is within the safe level for human body [32]. The output voltage on the 50 Ω load of the capsule antenna is calculated from the numerical modeling. It is known from the calculation that 2.70 mW wireless power can be received by the implanted antenna with AF-WPT,

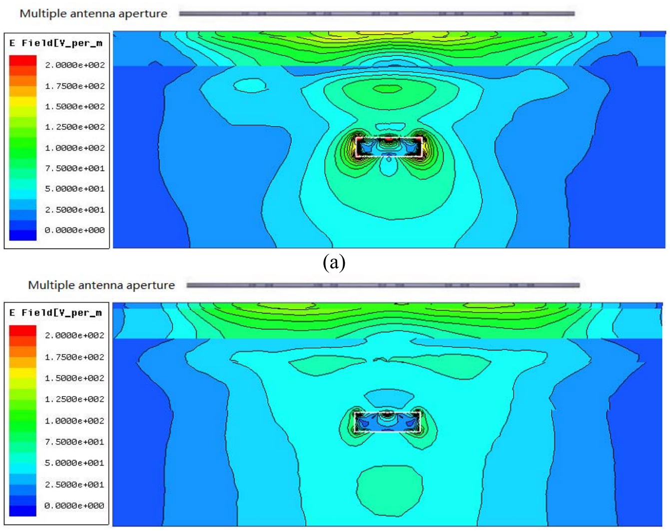

Fig. 8. Field intensity distribution in profile of layered tissues. (a) Field resulted from focused feeding. (b) Field resulted from equiphase feeding.

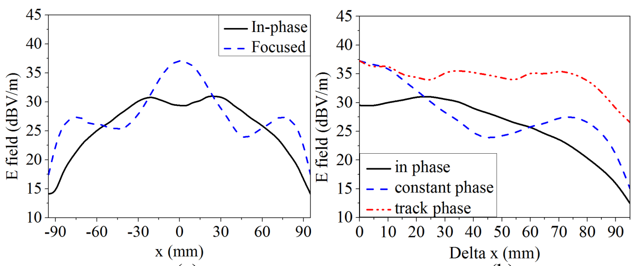

Fig. 9. (a) Distribution of field intensity along x-axis when the central of the radiation aperture locates at point X = 0, the capsule antenna locates at (0, 0, 50). The blue dashed line and black line stand for AF feeding and in-phase feeding, respectively. (b) Variation of field intensity at position of capsule with its moving along axis x. The black solid, blue dashed, and red dashed dotted lines stand for the results of the three feeding schemes, respectively.

showing 0.54% of the total transmission efficiency. On the contrary, only 0.14% of the total transmission efficiency has been obtained by radiation array with homogeneous feeding.

B. Influence of Device Shifting on WPT Efficiency

The implanted medical device may keep shifting in the body tissues (in the digestive tract, for example). Assume the field components are focused first on the initial position of the implanted antenna by means of pretesting and adjusting the phase of multiple antennas. Then, the implanted antenna shifts from the initial position (0, 0, 50) gradually, and finally to the endpoint (90, 0, 50). Keeping the program of the pretest and the adaptive focusing going on in the entire moving process, one can get the curve of the focused field intensity at different locations of the implanted antenna with different displacements in the x-direction, as shown in Fig. 9(b). The red dashed-dotted curve, the blue dash curve, and the black solid curves in this Fig. 9(b) correspond to the cases of feeding with the adaptive focusing in the entire track, the adaptive focusing only at the start point of the track, and the homogeneous feeding invariant in the entire moving track, respectively. It can be easily found from Fig. 9 that the electric field intensity in all the locations of implanted antenna in the first case is much stronger and more stable with the moving of implanted antenna than in the other cases, showing remarkable improvement of the WPT efficiency by using the adaptive focusing in the entire track. That is to say, the focused region of the field can be shifted continuously and always coincides with the surface of the implanted antenna. This is a really important performance when the capsule endoscope keeps moving in the digestive tract and its positions are always unknown.

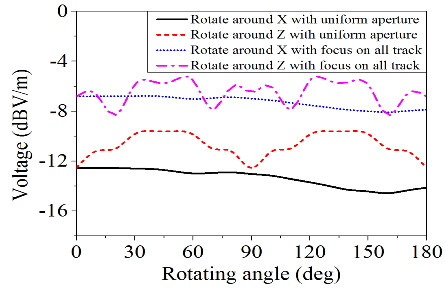

Fig. 10. Variation of received signal voltage on 50 Ω load with the rotation of capsule antenna, where 0 dB corresponds to 1 V. The original orientation of the capsule is shown in Fig. 3(b).

C. Influence of Device Rotation on WPT Efficiency

Actually, the capsule antenna has the most intensive response to the incident wave only when the direction of the wave polarization coincides with the axis of the capsule because the antenna is basically a dipole in the direction of the capsule axis. However, the orientation of the capsule and the principal polarization direction of the capsule antenna are difficult to be identified in real time due to the possible rotation of the capsule when it is moving along digestive tract down. Therefore, the polarization mismatching between the antennas outside body and the capsule antenna inside body seems to be unavoidable. Fortunately, the AF-WPT is able to match the polarizations adaptively.

In the pretest step, the intensities of signals received by the antenna ports with their polarization matched to that of the implanted antenna are higher than that in the mismatched cases. Consequently, only the antenna ports with the matched polarization, as the transmission terminals of the effective propagation channels, have been fed with the same intensive power in the WPT step. As a result, the much higher transmission efficiency has been got for AF-WPT compared to that in cases without using AF scheme.

It is assumed that the radiation aperture of the multiple antennas outside human body and therefore the principal polarizations of its field are all parallel to xy plane (also the body surface). The variation of the signal voltage on 50 Ω load of the capsule antenna as it rotates in xy plane is shown in Fig. 10. It can be seen from Fig. 10 that the signal obtained by this AF scheme is much more intensive than that in case of uniform phase feeding. It is because the AF scheme is able to adjust the wave polarization adaptively to the main polarization direction of the capsule antenna with rotation in the xy plane. In other words, the AF method has shown its performances of the adaptions not only for the location but also for the

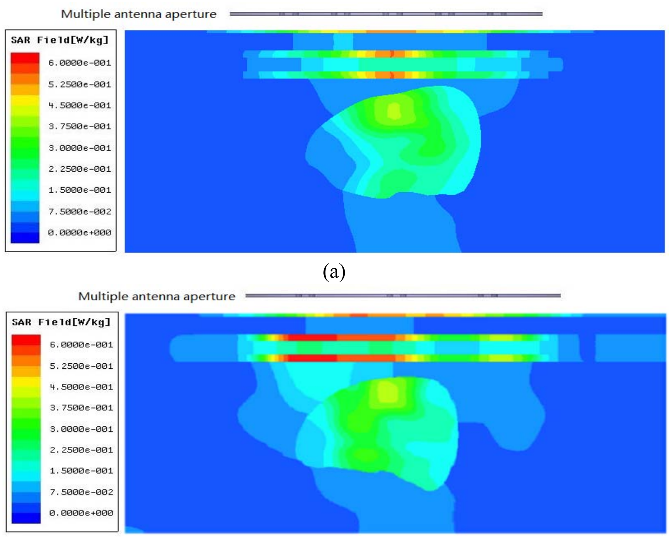

Fig. 11. SAR distribution in the abdominal cavity resulted from illumination of AF WPT. (a) SAR in *yz* plane. (b) SAR in *xz* plane.

principal polarization of the implanted antenna for its moving and rotation.

D. SAR Distribution and Radio Safety

There are many studies about the specific absorption rate (SAR) limitation for WPT to implanted devices in the previous work, for example the discussion in [20]. The numerical results of the SAR distribution in human body have also been given here to show the radiation safety of the AF-WPT scheme.

SAR is defined as the EM energy absorbed by unit volume of a given medium per unit time. SAR is proportional to the field intensity and the conductivity of the medium, and can be expressed as

$$\mathrm{SAR} = \frac{\sigma E^2}{2\rho} \tag{4}$$

where σ, E, and ρstand for the conductivity of the medium, the intensity of the electrical field, and the density of the medium, respectively. SAR can be easily calculated according to the specification in [20], once the intensity of the electrical field in the tissue of human body is obtained from the numerical modeling or the experimental measurement.

Fig. 11(a) and (b) shows the profiles of SAR distribution in the yz plane with $x = 0$, and in the xz plane with $y = 0$, respectively, all obtained from the numerical modeling, where x, y, and z stand for the direction of the height, the width, and the depth of the human body, respectively. The variation of SAR amplitude with the depth increasing is shown in Fig. 12 where the standard of SAR limitation has also been given for comparison. It can be easily seen from Fig. 12 that SAR is in the safety range and far below the threshold of the American FCC standard when human abdominal cavity is illuminated by 500 mW of EM power with 2.45 GHz for adaptive focusing WPT. It is also shown that SAR level is still not higher than the threshold of the American standard even 1000 mW of EM energy has been applied as the source of the AF-WPT. The "other standard" in Fig. 12 means the SAR

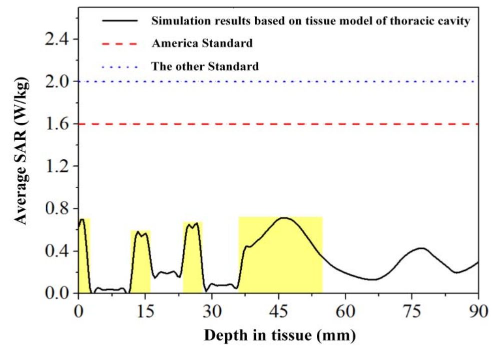

Fig. 12. Variation of SAR with the depth of tissue in the abdominal cavity, where the black solid line, the red dashed line, and the blue point line stand for the results of numerical simulation, the threshold of American Standard, the threshold of ICNIRP'AIEEE, and EN standard, respectively.

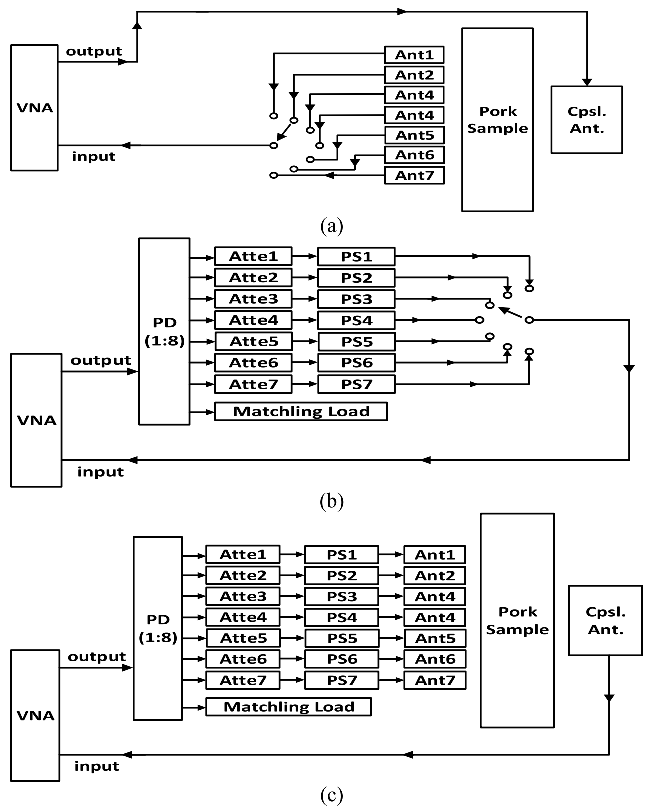

Fig. 13. Experimental scheme of adaptive focusing WPT. (a) Pretest scheme for measuring phase delay and field attenuation of each channel. (b) Channel tuning for given phase leading and amplitude of feedings to each antenna element. (c) Implementation of adaptive focusing WPT and measurement of focusing field.

standard of International Commission on Non-Ionizing Radiation Protection (ICNIRP), IEEE, and EN (Europe Standard).

V. Experiment for Adaptive Focusing WPT

In this paper, an experiment has been given to show the validation and the performance of the adaptive focusing WPT method. The experimental scheme is shown in Fig. 13 where the radio source is provided by a vector network analyzer (VNA) Keysight N9913A, and a 1–8 power divider has been used to feed the seven antenna elements and a 50 Ω

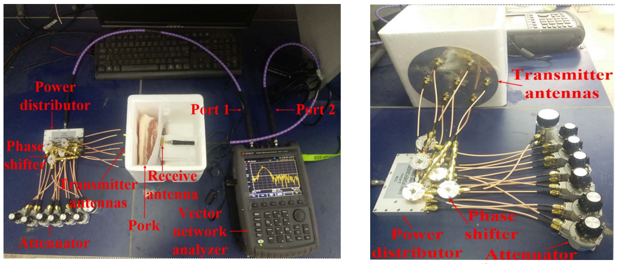

(a) (b)

Fig. 14. Experimental setup for adaptive focusing WPT. (a) Equipment connection. (b) Circuit with attenuators, shifters, and multiantennas' aperture.

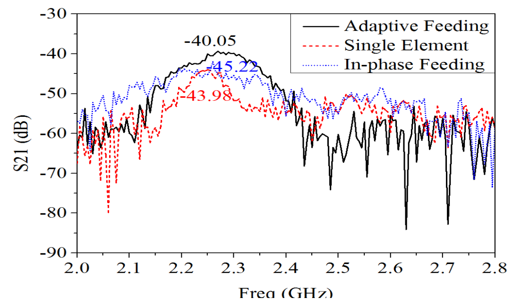

Fig. 15. Experimental results of adaptive focusing WPT, where the black solid line, the red dashed line, and the blue dashed line represent results of WPT with the AF feeding, single antenna feeding, and in-phase array feeding.

matching load, respectively. There are three basic steps in the experiment. As the first step, the pretest is implemented to measure the phase delay of each wireless channel. Fig. 13(a) represents the system scheme of the pretest for measuring the phase delays of the signals received by the 14 antenna ports (two ports for each antenna). The implanted antenna is fed by the source in the VNA first. The wave radiated by the implanted antenna propagates through the block of the pork, and is finally received by the 14 ports of the seven antennas outside body. The phase delays of the signals received by the 14 ports have all been measured and recorded by VNA, respectively.

Step 2 is designed for preadjustment of the seven channels before the WPT step. In step 2, the amplitude attenuator and the phase shifter of each feeding channel are all adjusted carefully to set their value consistent with the data in step 1, particularly set the phase conjugated to that obtained from the pretest. Let the power signals from the output port of the VNA transmit through the power divider, the attenuator, and the phase shifter in each channel successively, and finally arrive at the input port of the analyzer, respectively, as shown in Fig. 13(b). Adjust the phase shifter and the attenuator in each channel carefully until the phase delay and the amplitude attenuation of the signals in each channel shown in the VNA meet the values required for the adaptive focusing.

In step 3, the adaptive focusing of WPT is implemented and the gain of the signal intensity at the position of the implanted antenna is measured. As shown in Fig. 13(c), the power signals, transmitting through the power divider and the seven feeding channels adjusted in step 2, exciting the corresponding antenna elements with the proper phase leading and the amplitude, are finally radiated into the tissue, respectively. Transmitting through the body tissues, all the wave components radiated from the seven antenna elements are superimposed in-phase at the position of the implanted antenna because the absolute value of phase lead is equal to that of phase delay obtained in step 1, making a perfect phase compensation.

The experimental setup is shown in Fig. 14 where the equipment connection is shown in Fig. 14(a), and the circuit with the attenuators, the shifters, and the aperture of the multiple antennas is shown in Fig. 14(b).The block of the pork is positioned in a plastic box for convenience of fixing and measurement. The aperture of the multiple antennas, separated by the plastic box wall, clings to the pork block, as shown in Fig. 14(b). Both the multiple antennas and the "implanted" antenna are designed to match their feeding line perfectly at the same operating frequency. The thickness of the pork is 50 mm, and the aperture of the multiantennas is separated with 10 mm from the pork surface, and the "implanted" antenna is located also 10 mm from the pork muscle inside the box. The experiments with three kinds of feedings, i.e., the feeding with adaptive focusing, the feeding by single antenna element, and the in-phase feeding, are all implemented, respectively, under the excitation with the same total power, and the signal levels received by the "implanted" antenna in those three cases have all been measured for comparison.

The experimental results are represented in Fig. 15 where the black solid line, the red dashed line, and the blue dotted line represent the results of WPT with the AF feeding, the single antenna feeding, and the in-phase feeding, respectively. It can be seen from Fig. 15 that the field intensity at the position of the implanted antenna when using AF feeding is 5.17 dB higher than that when using the in-phase feeding, and 3.93 dB higher than that when using the single antenna feeding, all under the excitation of the same total power. It is evident from the experimental results that the AF method has much higher transmission efficiency and the 5.17 dB of the efficiency improvement is very similar to the 6 dB numerical results. The small difference may be caused by the difference between the perfectly layered media used in the numerical model and the block of the pork used in the experiment.

VI. Discussions and Conclusion

A novel method for WPT in complex multipath environment of human body has been proposed in this paper to adaptively enhance the intensity of the field on the surface of the implanted antenna. Both the numerical model and the experimental setup with multiple antennas out of body and implanted antenna inside the tissue have been built. It has been shown from the numerical modeling and the experimental measurement that the AF-WPT scheme enhances the intensity of the field on the surface of the implanted antenna inside the tissue about 6 dB higher than other methods, and the level of the received power is stable with the continuous shifting of the medical device along the digestive tract.

As we all know, the propagation of the EM waves through the human body, which is dependent on different sizes and figures of different people, is a very complex process with the multipath scattering, and different positions and orientations of the moving medical device make the process more difficult to be described and evaluated previously. Therefore, the various model-dependent WPT schemes are doomed to face a lot of severe challenges. By contrast, the novel model-independent WPT method with AF scheme proposed in this paper, simply based on the reciprocity theorem and the two-way communication of the implanted devices, can deal well with all the challenges mentioned above. Obviously, the proposed WPT scheme is adaptive both for different sizes and figures of human body, and for different locations and orientations of implanted antennas. Therefore, it is a universal WPT scheme for most medical applications.

Furthermore, the AF method results in the strong intensity of the field only on the surface of the implanted antenna. On the contrary, the field intensity in area around the antenna is very weak, and fully meets the SAR safety standard. In other words, the field focus scheme does not result in any potential hurt to the surrounding tissue. Moreover, the more complex the inhomogeneity of the propagation media, the more remarkable the multipath effect appears, and the stronger the field focus effect is. This is one more advantage of the AF scheme for WPT applications.

Finally, the increment of the technique complexity resulted from the adaptive field focusing is limited to the design of the multiple antennas and their feeding system outside human body, and nothing to do with the implanted devices. In other words, the adaptive field focusing is very easy to be implemented.

It should be noted that the proposed AF WPT scheme can provide us with possibilities to improve WPT technology, optimizing the system design for instance. Actually, the optimum design includes the electrical size of the aperture of the multiple antennas, the spacing between the adjacent antennas, the distance of the aperture from the body surface, the introduction of the transition layer between the aperture and the body surface, and the electrical and geometrical parameters of the transition layer. It has been shown that the efficiency of the AF WPT has increased to 1.14% after the above measures are implemented. Considering the main topic and the length limitation of this paper, the optimum design will be discussed in the other paper.

References

[1] S. Kim, J. S. Ho, and A. S. Y. Poon, "Wireless power transfer to miniature implants: Transmitter optimization," *IEEE Trans. Antennas Propag.*, vol. 60, no. 10, pp. 4838–4845, Oct. 2012.

[2] J. Lee and S. Nam, "Fundamental aspects of near-field coupling small antennas for wireless power transfer," *IEEE Trans. Antennas Propag.*, vol. 58, no. 11, pp. 3442–3449, Nov. 2010.

[3] J.-R. Yang, H.-C. Son, and Y.-J. Park, "A class E power amplifier with coupling coils for a wireless power transfer system," *Prog. Electromagn. Res. C*, vol. 35, pp. 13–22, Nov. 2013.

[4] R. Bosshard, J. Mühlethaler, J. W. Kolar, and I. Stevanović, "Optimized magnetic design for inductive power transfer coils," in *Proc. IEEE 28th Annu. Appl. Power Electron. Conf.*, Mar. 2013, pp. 1812–1819.

[5] Y.-S. Seo, M. Q. Nguyen, Z. Hughes, S. Rao, and J.-C. Chiao, "Wireless power transfer by inductive coupling for implantable batteryless stimulators," in *IEEE MTT-S Int. Microw. Symp. Dig.*, Jun. 2012, pp. 1–3.

[6] A. Kurs, A. Karalis, R. Moffatt, J. D. Joannopoulos, P. Fisher, and M. Soljačić, "Wireless power transfer via strongly coupled magnetic resonances," *Science*, vol. 317, no. 5834, pp. 83–86, 2007.

[7] J. Gozalvez, "WiTricity—The wireless power transfer [mobile radio]," *IEEE Veh. Technol. Mag.*, vol. 2, no. 2, pp. 38–44, Jun. 2007.

[8] Z. Wang, X. Wei, and H. Dai, "Principle elaboration and system structure validation of wireless power transfer via strongly coupled magnetic resonances," in *Proc. IEEE Vehicle Power Propuls. Conf. (VPPC)*, Oct. 2013, pp. 1–6.

[9] X. Zhang, S. L. Ho, and W. N. Fu, "Quantitative analysis of a wireless power transfer cell with planar spiral structures," *IEEE Trans. Magn.*, vol. 47, no. 10, pp. 3200–3203, Oct. 2011.

[10] S. Konno, T. Yamamoto, and K. Koshiji, "Improvement of coupling coefficient by designing a spiral pattern formed on a printed circuit board," in *Proc. IEEE Wireless Power Transf. (WPT)*, May 2013, pp. 167–170.

[11] K. Miwa, H. Mori, N. Kikuma, H. Hirayama, and K. Sakakibara, "A consideration of efficiency improvement of transmitting coil array in wireless power transfer with magnetically coupled resonance," in *Proc. IEEE Wireless Power Transf.*, May 2013, pp. 13–16.

[12] I. Awai, Y. Sawahara, and T. Ishizaki, "Choice of resonators for a WPT system in lossy materials," in *Proc. IEEE Wireless Power Transf. Conf. (WPTC)*, May 2014, pp. 106–109.

[13] O. Jonah, Stavros V. Georgakopoulos, D. Daerhan, and S. Yao, "Misalignment-insensitive wireless power transfer via strongly coupled magnetic resonance principles," in *Proc. IEEE Antennas Propag. Soc. Int. Symp. (APS/URSI)*, Jul. 2014, pp. 1343–1344.

[14] O. Jonah, S. V. Georgakopoulos, and M. M. Tentzeris, "Orientation insensitive power transfer by magnetic resonance for mobile devices," in *Proc. IEEE Wireless Power Transf. (WPT)*, May 2013, pp. 5–8.

[15] H. Mei and P. P. Irazoqui, "Miniaturizing wireless implants," *Nature Biotechnol.*, vol. 32, pp. 1008–1010, Oct. 2014.

[16] A. S. Y. Poon, S. O'Driscoll, and T. H. Meng, "Optimal frequency for wireless power transmission into dispersive tissue," *IEEE Trans. Antennas Propag.*, vol. 58, no. 5, pp. 1739–1750, May 2010.

[17] M. Ma and A. S. Y. Poon, "Midfield wireless power transfer for bioelectronics," *IEEE Circuits Syst. Mag.*, vol. 15, pp. 54–60, 2nd Quart., 2015.

[18] J. S. Ho, S. Kim, and A. S. Y. Poon, "Midfield wireless powering for implantable systems," *Proc. IEEE*, vol. 101, no. 6, pp. 1369–1378, Jun. 2013.

[19] S. Kim, J. S. Ho, and A. S. Y. Poon, "Midfield wireless powering of subwavelength autonomous devices," *Phys. Rev. Lett.*, vol. 110, no. 20, pp. 1369–1378, 2013.

[20] J. S. Ho *et al.*, "Wireless power transfer to deep-tissue microimplants," *Proc. Nat. Acad. Sci. USA*, vol. 111, no. 22, pp. 7974–7979, Apr. 2014.

[21] J. Loane, H. Ling, B. F. Wang, and S. W. Lee, "Experimental investigation of a retro-focusing microwave hyperthermia applicator: Conjugate-field matching scheme," *IEEE Trans. Microw. Theory Techn.*, vol. 34, no. 5, pp. 490–494, May 1986.

[22] M. Fink, C. Prada, F. Wu, and D. Cassereau, "Self focusing in inhomogeneous media with time reversal acoustic mirrors," in *Proc. IEEE Ultrason. Symp.*, Oct. 1989, pp. 681–686.

[23] G. Lerosey, J. de Rosny, A. Tourin, A. Derode, G. Montaldo, and M. Fink, "Time reversal of electromagnetic waves," *Phys. Rev. Lett.*, vol. 92, no. 19, p. 193904, May 2004.

[24] G. Lerosey, J. de Rosny, A. Tourin, A. Derode, and M. Fink, "Time reversal of wideband microwaves," *Appl. Phys. Lett.*, vol. 88, no. 15, p. 154101, 2006.

[25] J. de Rosny, G. Lerosey, and M. Fink, "Theory of electromagnetic time-reversal mirrors," *IEEE Trans. Antennas Propag.*, vol. 58, no. 10, pp. 3139–3149, Oct. 2010.

[26] C. A. Balanis, *Advanced Engineering Electromagnetics*, 2nd ed. Hoboken, NJ, USA: Wiley, 2012, pp. 323–325.

[27] N. Zaiping, Y. Yang, and Z. Xianzheng, "Wireless charging method and apparatus based on radio frequency receiving and phase compensation retransmission," U.S. Patent 15 387 813, Jan. 4, 2017.

[28] S. Gabriel, R. W. Lau, and C. Gabriel, "The dielectric properties of biological tissues: III. Parametric models for the dielectric spectrum of tissues," *Phys. Med. Biol.*, vol. 41, no. 11, p. 2271, 1996.

[29] D. Andreuccetti, R. Fossi, and C. Petrucci, "An Internet resource for the calculation of the dielectric properties of body tissues in the frequency range 10 Hz-100 GHz," in *Proc. IFAC-CNR*, Florence Italy, 1997. [Online]. Available: http://niremf.ifac.cnr.it/tissprop/

[30] J. Ma, J.-M. Jin, and Z. Nie, "A nonconformal FEM-DDM with tree–cotree splitting and improved transmission condition for modeling subsurface detection problems," *IEEE Trans. Geosci. Remote Sens.*, vol. 52, no. 1, pp. 355–364, Jan. 2014.

[31] M. Jin and N. Zaiping, "FEM-DDM with an efficient second-order transmission condition in both high-frequency and low-frequency applications," *Prog. Electromagn. Res. B*, vol. 50, pp. 253–271, Apr. 2013.

[32] R. Das and H. Yoo, "Biotelemetry and wireless powering for leadless pacemaker systems," *IEEE Microw. Wireless Compon. Lett.*, Vol. 25, pp. 262–264, Apr. 2015.

[33] Z. Nie and Y. Yang, "A wireless charging method and device based on radio frequency receiving and phase compensation forwarding," CN Patent 201 610 218 755.8, Jul. 13, 2016.

Zaiping Nie (SM'96–F'12) was born in Xi'an, China, in 1946. He received the B.S. degree in radio engineering and the M.S. degree in electromagnetic field and microwave technology from the University of Electronic Science and Technology of China, Chengdu, China, in 1968 and 1981, respectively.

He is currently a Professor with the Department of Microwave Engineering, UESTC. From 1987 to 1989, he was a Visiting Scholar with the Electromagnetics Laboratory, University of Illinois, Urbana, IL, USA. He has authored or co-authored over 400 journal papers. His current research interests include computational electromagnetics and its applications, antenna theory and techniques, electromagnetic scattering and inverse scattering, and field and waves in inhomogeneous media.

Yuan Yang was born in Qujing, China, in 1992. He received the B.S. and M.S. degrees in electromagnetic field and wireless technology from the University of Electronic Science and Technology of China, Chengdu, China, in 2014 and 2017, respectively.

His current research interests include wireless power transfer, antennas, and arrays.